Applied Physics B (2022) 128: 168
https://doi.org/10.1007/s00340-022-07889-6

Applied Physics B
Lasers and Optics

Compression of attosecond water window pulse by stacked Cr/Sc multilayer mirror with chirped structure

Chengyou Lin[1] · Taolve Yang[1] · Shujing Chen[2]

Received: 24 January 2022 / Accepted: 4 August 2022 / Published online: 14 August 2022

Abstract
An attosecond water window pulse generated from high harmonics spectrum is chirped, and needs to be compressed to transform limited pulse by chirp compensation. In this paper, a Cr/Sc-stacked multilayer with chirped structure is proposed for attosecond pulse compression. Three stacked multilayer mirrors are designed to compress chirped attosecond pulses covering 300–400 eV water window spectrum. Nearly, transform limited attosecond pulses are all obtained after reflected by the stacked multilayer mirrors, which exhibit 0.27%, 0.41%, and 0.58% average reflectivity and − 2086, − 3481 or − 5644 as^2 average group delay dispersion in the 300–400 eV region, respectively. The research proposes a stacked multilayer mirror for chirp compensation and pulse compression, which could be used for pulse shaping of an attosecond water window pulse.

1 Introduction

As an efficient tool for observing and controlling electron dynamics in atoms, molecules and condensed matter, attosecond pulses keep the one of most active frontiers in ultrafast science, and continue to attract growing attentions in the last two decades [1, 2]. Recent advances in the development of attosecond sources extends from the extreme ultraviolet to the water window spectral range [between the atomic K-shell excitation of carbon (284 eV) and oxygen (543 eV)] [3, 4], which enables the generation of ever shorter attosecond pulses [5, 6], and allows to access deeper electron core levels that may facilitate the investigation of biomolecules and cells in femtosecond and attosecond time-resolved soft X-ray microscopy experiments [7, 8].

At present, high-harmonic generation (HHG) [9, 10] is the dominating method for generating attosecond pulses. However, it is well known that attosecond pulses emanating from short trajectory harmonics are positively chirped [11, 12], resulting in significant pulse broadening. The value of chirp (atto-chirp) at the center of the plateau region of the high-harmonic spectrum is inversely proportional to the peak intensity and central wavelength of the driving laser, which is around thousands as^2 for HHG in the water window region according to the semi-classical three-step model [13]. Thin metallic filters with negative group delay dispersion are generally used to compensate the positive chirp of attosecond pulses in the wavelength below 300 eV [14–16]. However, for compensation the atto-chirp beyond 300 eV, it is hard to find appropriate materials that have sufficient dispersion with high transmission [17].

A chirped multilayer mirror with a spatial variation of the layer thickness is a key component for attosecond pulses shaping [18], and has been applied for chirped compensation and pulse compression of attosecond pulses in the extreme ultraviolet (EUV) [19–24], soft X-ray [25, 26] and hard X-ray [27] regimes. The basic idea of a chirped multilayer mirror is that the Bragg wavelength is not constant but varies within the structure, so that light at different wavelengths penetrates to a different extent into the mirror structure and thus experiences a different group delay. The chirp compensation of chirped mirrors is not dependent on material dispersion, but relies on multilayer mirror reflections to build up the phase delay difference for different photons, and can, therefore, be applied to a wider range of wavelengths.

In general, the achievement of broadband chirp compensation together with high reflection is required for a chirped mirror, which needs to optimize the thickness of each layer in the multilayer structure (i.e., aperiodic multilayer) [28].

✉ Chengyou Lin
cylin@mail.buct.edu.cn

✉ Shujing Chen
chenshujing@cugb.edu.cn

[1] College of Mathematics and Physics, Beijing University of Chemical Technology, Beijing 100029, China

[2] School of Materials Science and Technology, China University of Geosciences, Beijing 100083, China

The structural optimization of a EUV chirped mirror is not hard because the number of optimized layers is not too many (e.g., dozens of bilayers for a Mo/Si multilayer). However, when photon energy increases from the EUV region to the water window region, the difference of refractive index of paired materials becomes smaller, and the achievement of high reflectivity needs more bilayers [29]. Cr/Sc multilayer is widely used in the water window region, which can provide sufficient reflectivity, and achieve a pulse profile which is closer to Fourier limit in time and frequency domains [18]. In particular, for a Cr/Sc multilayer, several hundreds of Cr/Sc bilayers are generally required for achieving high reflectivity in the water window region [30]. For designing a chirped multilayer mirror, the usage of more layers in the multilayer means optimizing more parameters, leading to low optimization efficiency.

A stacked multilayer mirror is a type of aperiodic multilayer composed of several periodic multilayer stacking in sequence, which also realizes broadband reflection. The freedom degree (designable structural parameter) of a stacked multilayer mirror is obviously less than an aperiodic multilayer with distinct thickness for each layer, making it advantageous in both theoretical design and practical preparation. Barysheva et al. used Mo/Si [31] or Mo/Be [32] stacked multilayer mirrors to achieve 16% or 13% uniform reflectivity in the EUV region of 17–21 nm or 11.1–13.8 nm, respectively. Yao et al. used stacked (also called block) multilayer mirrors to achieve mean reflectivity over 15% in the super broad hard X-ray region of 45–60 keV [33]. Recently, we used a Cr/Sc-stacked multilayer mirror to design a broadband reflector in the water window region, and it exhibited better optimization efficiency, design robustness, and thickness error tolerance than an aperiodic multilayer mirror [34]. Until now, a stacked structure-based chirped mirror has not been proposed for an attosecond pulse compression.

In this paper, a stacked Cr/Sc multilayer mirror is proposed, and used for attosecond pulses' compression in the water window region. The design method of proposed stacked multilayer mirror with linearly chirped structure [35] is presented. Using this method, the stacked multilayer mirrors for compressing attosecond water window pulses with different chirps are designed. Theoretical analysis in time domain and frequency domain are carried out, and the performances of designed stacked multilayer mirrors are investigated.

2 Theory

2.1 Stacked structure

The proposed stacked multilayer is composed of several periodic Cr/Sc multilayers in sequence as shown in Fig. 1.

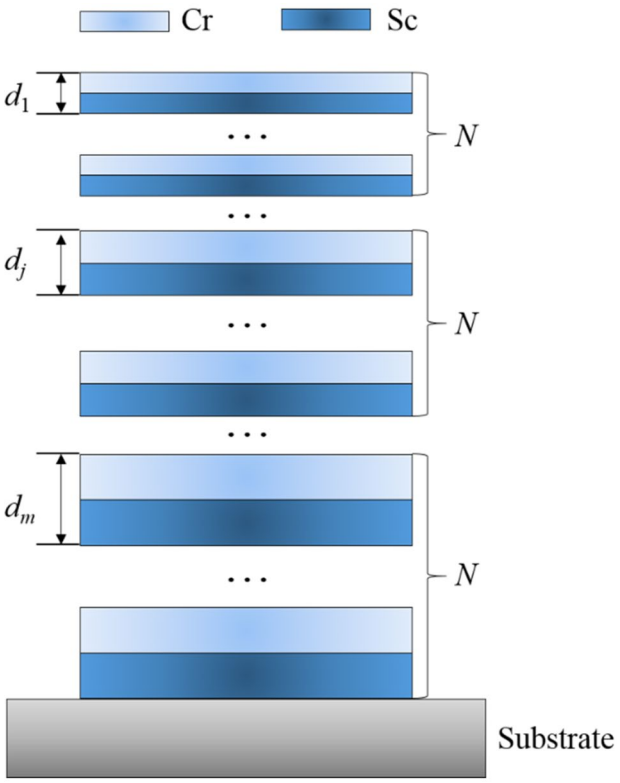

Fig. 1 Stacked Cr/Sc multilayer with chirped structure

Structural parameters such as the number of periodic multilayers (m) in the stacked multilayer and the bilayer number (N_j), bilayer thickness (d_j) and thickness ratio (γ_j) for each periodic multilayer are designed ($j = 1-m$). To simplify the design process, N_j and γ_j are assumed to be the same value (N, γ) for each periodic multilayer. In addition, $m = 10$ are $\gamma = 0.5$ are used for the proposed stacked multilayer. In this case, N and d_j are considered to be the main design objects.

2.2 Design method

The phase relation between harmonics is not linear, but there exists a time delay of harmonics (positive chirp) that broadens the duration of the attosecond pulse [36]. A negative time delay between low- and high-energy photons can be introduced by Bragg reflection of a multilayer with chirped structure to compensate such positive chirp for obtaining a transform limited pulse in time domain. Such chirped multilayer mirrors generally exhibit negative group dispersion delay (GDD) in the frequency domain of incidence pulse. In our design, the highest energy photon is reflected by the top periodic multilayer in the stacked structure, while the lowest energy photon is reflected by the bottom one to achieve negative GDD. Therefore, the bilayer thickness of the first (d_1) or the last (d_m) periodic multilayer can be set to be the half wavelength of the starting (λ_1) or ending wavelength (λ_2), respectively, in

the high-harmonic spectrum to fulfill Bragg condition. $\{d_j\}$ ($j=1-m$) is set to be an arithmetic sequence as follows:

$$d_j = d_1 + \frac{j-1}{m-1}\left(d_m - d_1\right).(j = 1-m) \tag{1}$$

In Eq. (1), the bilayer thickness of periodic multilayer in the proposed stacked structure linearly increases from top to bottom to form a linearly chirped structure. By this way, the light with short wavelength (high-energy photon) is reflected frontally, while the light with long wavelength (low-energy photon) is reflected later, inducing a negative GDD that can compensate the intrinsic positive GDD due to the incident pulse entering the reflection bandwidth in the frequency domain. However, to completely compensate the GDD of incident spectrum, the values of negative GDD and the positive GDD should be the same, to obtain the transform limited pulse. Therefore, it is feasible to compensate for the intrinsic spectral chirp of the incident pulse over the entire reflection bandwidth using the GDD of the chirped mirror [37], which can be realized by choosing suitable number of periodic multilayer (N) in the proposed stacked structure:

$$2 \times N \times \sum_{j=1}^{m} d_j = \text{chirp} \times \Delta E \times c, \tag{2}$$

where *chirp* denotes the intrinsic positive chirp with unit of as/eV (1 as/eV = 658.2 as^2). ΔE represents the bandwidth of incident spectrum with unit of eV, and c is the light speed. For a chirped attosecond pulse, the main desirable parameters of proposed stacked multilayer such as N and $\{d_j\}$ can be determined directly by Eqs. (1) and (2).

2.3 Performance parameters

To analyze reflection performance of the proposed stacked multilayer mirror, the spectral complex reflection coefficient $r(\omega)$ needs to be determined first, using a standard matrix method based on the Fresnel equations [38]. The optical constants of Cr and Sc used in the simulations are derived from the handbook edited by Henke et al. [39]. Basing on $r(\omega)$, the spectral reflectivity $R(\omega)$, phase $\varphi(\omega)$, and GDD(ω) of the proposed stacked multilayer can be calculated as follows:

$$R(\omega) = |r(\omega)|^2, \tag{3}$$

$$\varphi(\omega) = \arctan\left(\frac{\text{Im}(r(\omega))}{\text{Re}(r(\omega))}\right), \tag{4}$$

$$\text{GDD}(\omega) = \frac{\partial^2 \varphi(\omega)}{\partial \omega^2}. \tag{5}$$

Using the complex reflection coefficient $r(\omega)$ calculated in frequency-energy domain, we can obtain the Fourier components of reflected attosecond pulse $E_1(\omega)$ by multiplying $r(\omega)$ with each Fourier component $E_0(\omega)$ of incident pulse ($E_1(\omega) = E_0(\omega)r(\omega)$), in which $E_0(\omega)$ can be obtained from the incident pulse field $E_0(t)$ by Fourier transform. Then, the inverse Fourier transform is performed on $E_1(\omega)$ to obtain the reflected pulse field $E_1(t)$ and intensity $I_1(t)$ ($I_1(t) = E_1(t)E_1^*(t)$). FWHM (full width at half maximum) of temporal pulse is used to evaluate pulse width for incident and reflected pulses (FWHM = $\delta_{0.5}$). To evaluate the reflection coefficient of the stacked multilayer for an attosecond pulse, a temporal parameter called power reflection coefficient R_P defined as the peak intensity ratio of reflected-to-incident pulse ($I_{1\max}/I_{0\max}$) is used [40]:

$$R_\text{p} = \frac{I_{1\,\max}}{I_{0\,\max}} = R\left(\frac{\tau_0}{\tau}\right), \tag{6}$$

in which τ_0 (or τ) is the duration of the incident (or reflected) pulses, and R is the reflected-to-incident pulse energy ratio, having the same value as the average reflectivity in the frequency domain:

$$R = \int_{-\infty}^{\infty} I_1(t)dt \Big/ \int_{-\infty}^{\infty} I_0(t)dt, \tag{7}$$

$$\tau_0 = \int_{-\infty}^{\infty} I_0(t)dt / I_{0\,\max}, \tag{8}$$

$$\tau = \int_{-\infty}^{\infty} I_1(t)dt / I_{1\,\max}. \tag{9}$$

3 Results and discussion

3.1 Design results

In the simulations, we use a smoothed flat-top shape spectral compositions covering 300–400 eV water window region to simulate the high-harmonic spectrum near the cutoff. Attochirps of 2000, 4000 and 6000 as^2 are considered in the spectrum, which are estimated according to the practical intensity and wavelength of the driving laser. Three stacked Cr/Sc multilayer mirrors with linearly chirped structure are designed for pulse compression of the chirped attosecond water window pulses.

Using the design method described above, the bilayer thickness of the first or the last periodic multilayer for each designed chirped mirror is the same, which is 1.549 or 2.066 nm. The bilayer thickness of middle eight periodic

multilayers can be obtained by Eq. (1). However, the bilayer number of periodic multilayer (N) of the designed stacked multilayer is different for attosecond pulse with distinct chirp. According to Eq. (2), N is calculated to be 3, 5 or 8 for atto-chirp of 2000, 4000 or 6000 as^2. The bilayer thickness distributions of three designed stacked multilayer mirrors are shown in Fig. 2. Although the bilayer thicknesses of the top and the bottom periodic multilayers are all the same for three stacked multilayers, the bilayer number of periodic multilayer increases with the chirp of incident pulse, indicating that larger chirp needs more layers to compensate.

3.2 Temporal analysis

To verify the pulse compression of designed stacked multilayers for incident chirped attosecond pulses, temporal profiles of incident, reflected and transform limited pulses for attosecond pulses with chirps of 2000, 4000 and 6000 as^2 are exhibited in Fig. 3. The simulated chirped attosecond pulse has a smooth flat-topped shape spectrum in the 300–400 eV range, and its Fourier transform limited pulse exhibits 36.65 as temporal width ($FWHM_{TL}$ = 36.65 as). However, the atto-chirp would broaden the pulses, and the temporal widths ($FWHM_0$) of incident attosecond pulses with 2000, 4000 and 6000 as^2 chirps are 210.06, 465.48 and 766 as, respectively, as listed in Table 1.

After reflected by stacked multilayer mirrors, it is seen that all chirped attosecond pulses are well compressed, and the temporal widths ($FWHM_1$) of reflected attosecond pulses are 37.61, 37.47 and 37.14 as, very close to the one of the transform limited pulse (36.65 as). It is demonstrated good performance of designed stacked multilayer mirrors for compressing chirped attosecond pulses, as shown in Fig. 3. High-order dispersions (such as third order dispersion) that cause pulse ripples are also introduced by multilayer reflection, but they are small and have little effect on temporal width and energy of attosecond pulse. In addition, the temporal pulse reflection efficiency is also investigated for the designed stacked multilayer mirrors. 1.22%, 3.34% and 6.80% power reflection coefficients are obtained for the incident pulse with 2000, 4000 and 6000 as^2 chirps, respectively. Increasing R_p with the atto-chirp is caused by more layers used in the respective stacked multilayer, which enhances Bragg reflection for the spectral compositions of incident pulses.

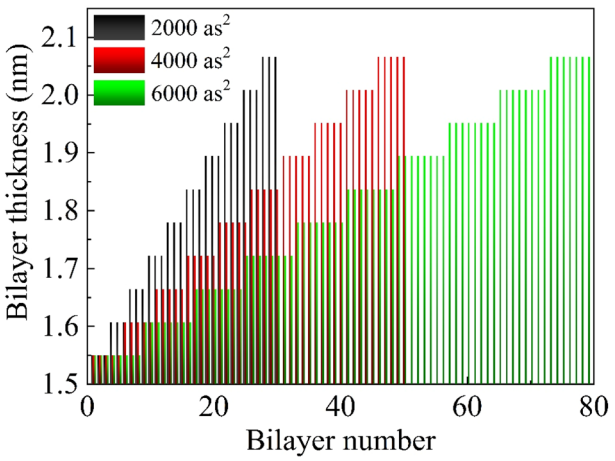

Fig. 2 Bilayer thickness distributions of three designed stacked Cr/Sc multilayer mirrors for attosecond pulse with chirps of 2000, 4000 and 6000 as^2

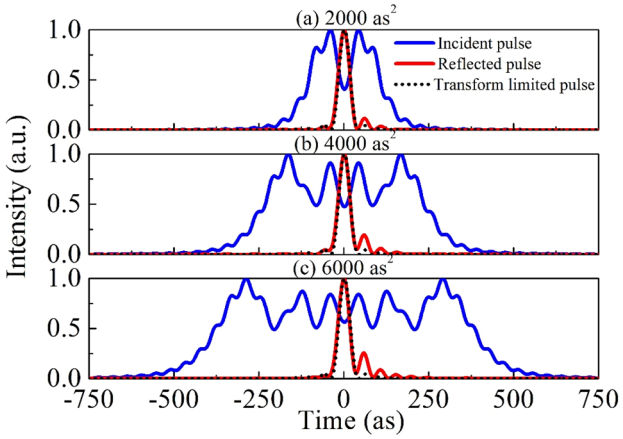

Fig. 3 Temporal profiles of incident, reflected and transform limited pulses for attosecond pulses with chirps of **a** 2000, **b** 4000 and **c** 6000 as^2

3.3 Spectral performance

To further investigate the physical mechanism of pulse compression of stacked multilayer mirrors, the spectral reflectivity and phase of three designed mirrors are plotted in Fig. 4. At first, all designed stacked multilayer mirrors exhibit broadband reflection in the spectral region from 300 to 400 eV, covering the compositions of incident pulses, as shown in Fig. 4a. Broadband reflection originates from the Bragg reflection of periodic multilayers in the stacked structure. Average reflectivity in the frequency domain in the 300–400 eV is 0.27%, 0.41% or 0.58% for the stacked mirror designed for the attosecond pulse with 2000, 4000 and 6000

Table 1 Temporal parameters of incident and reflected attosecond pulses

Atto-chirp/as^2	$FWHM_0$/as	$FWHM_1$/as	R_p (%)
2000	210.06	37.61	1.22
4000	465.48	37.47	3.34
6000	766.00	37.14	6.80

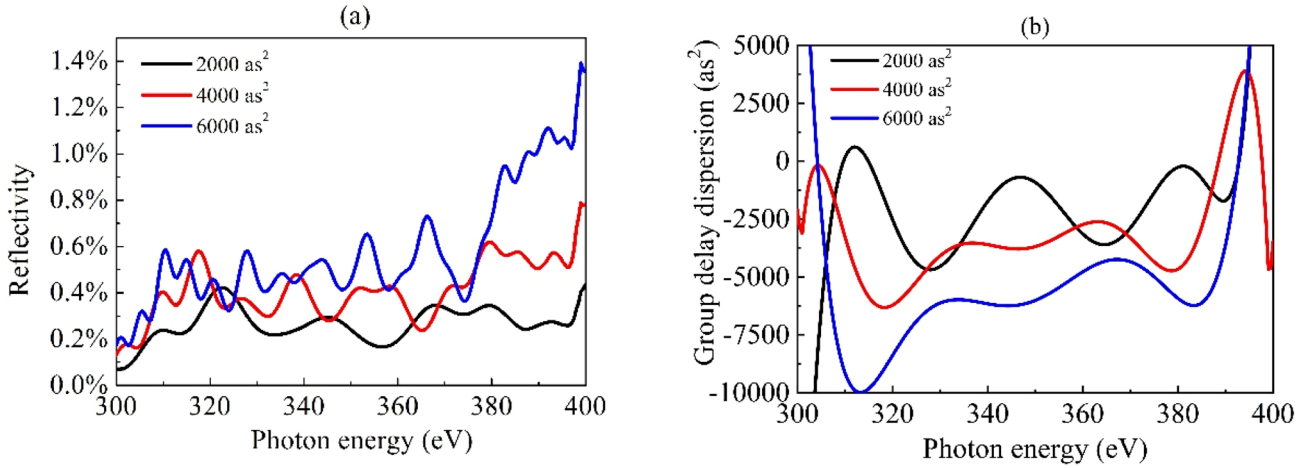

Fig. 4 **a** Reflective and **b** group delay dispersion of designed stacked Cr/Sc multilayer mirrors

as^2 chirps. The value of average reflectivity in frequency domain for each mirror is consistent with the ratio of the reflected-to-incident pulse energy in time domain.

Second, with the increase of photon energy, reflective phase presents a quadratic function curve with negative quadratic coefficient for each stacked mirror, indicating a negative group velocity delay which is designed for positive atto-chirp compensation, as shown in Fig. 4b. Average GDD in the 300–400 eV is − 2086, − 3481 or − 5644 as^2 for the stacked mirror designed for the attosecond pulse with 2000, 4000 or 6000 as^2 chirps. Tolerable deviation between GDD and atto-chirp comes from simplified process in the design method, such as estimated value of the number of periodic multilayer in the stacked multilayer, which does not affect the pulse compression effect. The origin of GDD ripples in chirped mirrors can be traced back to impedance mismatches of multilayer to ambient medium [41]. The unavoidable GDD oscillations may distort or broaden the time profile of the pulse [42].

Furthermore, we analyze the light intensity distributions inside the designed stacked Cr/Sc multilayer mirrors, as shown in Fig. 5. Spectral components with lower photon energy go deeper and reflected later than the ones with higher photon energy in each stacked structure, which is used to compensate the time delay of chirped pulse. With atto-chirp increases, the optical path between spectral components becomes large, which is used for compensating long delay formed by large chirp.

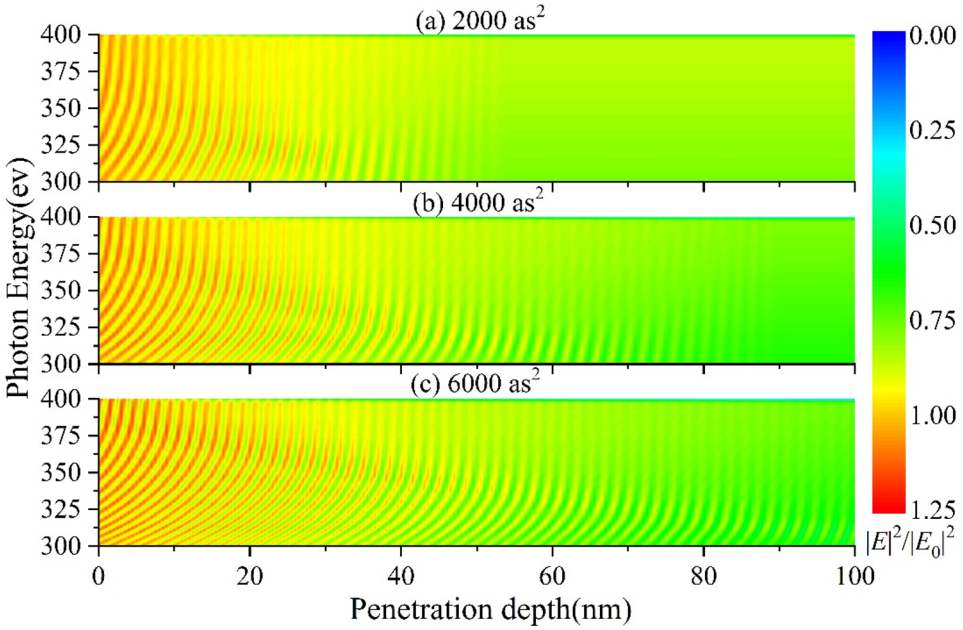

Fig. 5 Light intensity distributions inside the stacked Cr/Sc multilayer mirrors designed for attosecond pulses with chirps of **a** 2000, **b** 4000 and **c** 6000 as^2

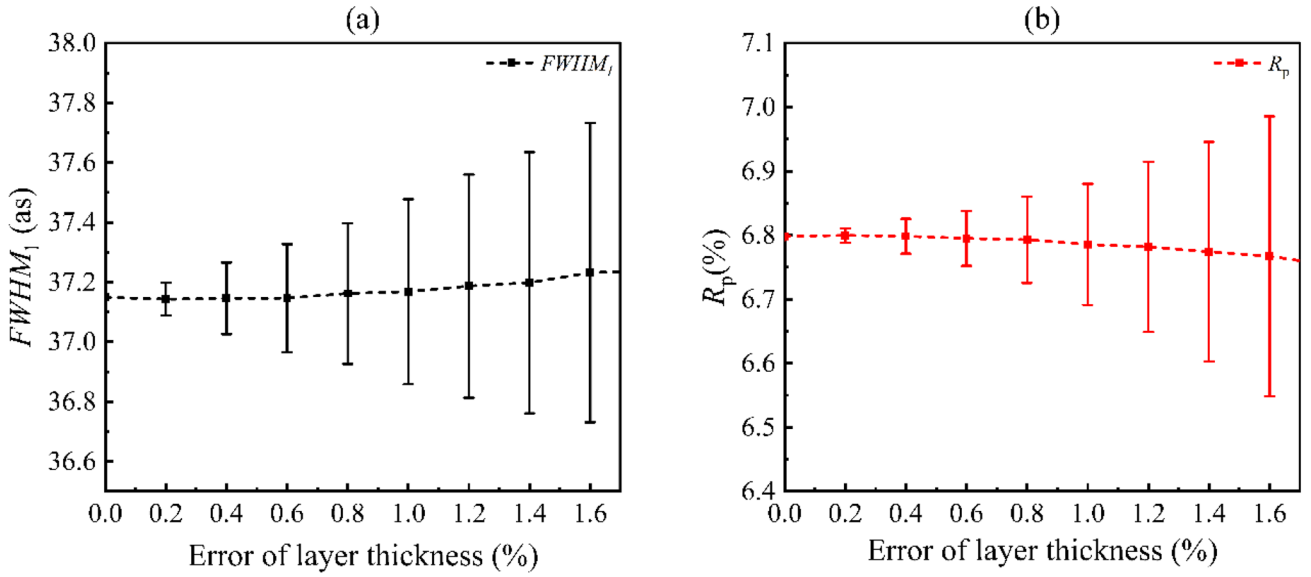

Fig. 6 **a** FWHM$_1$ and **b** R_p of designed stacked Cr/Sc multilayer mirrors for different layer thickness error

In order to investigate the effect of layer thickness error on the performance of designed stacked multilayer mirrors, two temporal parameters (FWHM$_1$ and R_p) of three stacked multilayer mirrors are calculated for different layer thickness errors. Random tests are conducted 100 times for each thickness error, and the results are shown in Fig. 6. The average value of FWHM$_1$ increases from 37.14 as to 37.23 as, and R_p decreases from 6.80 to 6.76% when the error of layer thickness varies from 0 to 1.6%. The small variation of FWHM$_1$ and R_p indicate good robustness of designed stacked multilayer mirror for layer thickness error, which makes it feasible in actual manufacturing.

4 Conclusion

In this paper, a design method of stacked multilayer mirror for attosecond pulse compression is present. Using this method, three stacked Cr/Sc multilayer mirrors with chirped structure are designed for pulse compression of attosecond water window pulses with 2000, 4000 and 6000 as^2 chirps. The temporal width of the chirped attosecond pulse is compressed from 210.06, 465.48 or 766 as to 37.61, 37.47 or 37.14 as, very close to the one of the transform limited pulse (36.65 as). Increasing power reflection coefficient with the atto-chirp is found, which is caused by more layers used in the stacked multilayer. Spectral reflectivity and group delay dispersion are also investigated for the stacked multilayer mirrors, and 0.27%, 0.41%, or 0.58% average reflectivity and − 2086, − 3481 or − 5644 as^2 average group delay dispersion in the 300–400 eV region is exhibited for the stacked mirror designed for the attosecond pulse with 2000, 4000 or 6000 as^2 chirp. By analyzing the light intensity distributions inside the designed stacked multilayer mirrors, spectral components with lower photon energy go deeper and reflected later than the ones with higher photon energy in each stacked structure. The optical path between spectral components becomes large with chirp increases, indicating the physical mechanism of stacked multilayer mirrors for chirp compensation and pulse compression. The research paves a way for attosecond water window pulse shaping, especially for the ones whose spectrum is beyond 300 eV, which is hard to achieve chirp compensation using material dispersion.

Funding This work was supported by the National Natural Science Foundation of China (61805007).

Declarations

Conflict of interest The authors declare that they have no known competing financial interests or personal relationships that could have appeared to influence the work reported in this paper.

References

1. P.B. Corkum, F. Krausz, Nat. Phys. **3**, 381 (2007)
2. F. Krausz, M. Ivanov, Rev. Mod. Phys. **81**, 163 (2009)
3. F. Silva, S.M. Teichmann, S.L. Cousin, M. Hemmer, J. Biegert, Nat. Commun. **6**, 6611 (2015)
4. X. Ren, J. Li, Y. Yin, K. Zhao, A. Chew, Y. Wang, S. Hu, Y. Cheng, E. Cunningham, Y. Wu, M. Chini, Z. Chang, J. Optics **20**, 023001 (2018)

5. S.M. Teichmann, F. Silva, S.L. Cousin, M. Hemmer, J. Biegert, Nat. Commun. **7**, 11493 (2016)
6. J. Li, X. Ren, Y. Yin, K. Zhao, A. Chew, Y. Cheng, E. Cunningham, Y. Wang, S. Hu, Y. Wu, M. Chini, Z. Chang, Nat. Commun. **8**, 186 (2017)
7. Y. Pertot, C. Schmidt, M. Matthews, A. Chauvet, M. Huppert, V. Svoboda, A. von Conta, A. Tehlar, D. Baykusheva, J.-P. Wolf, H.J. Worner, Science **355**, 264 (2017)
8. N. Saito, N. Douguet, H. Sannohe, N. Ishii, T. Kanai, Y. Wu, A. Chew, S. Han, B.I. Schneider, J. Olsen, L. Argenti, Z. Chang, J. Itatani, Phys. Rev. Res. **3**, 043222 (2021)
9. P.M. Paul, E.S. Toma, P. Breger, G. Mullot, F. Auge, P. Balcou, H.G. Muller, P. Agostini, Science **292**, 1689 (2001)
10. H. Yuan, L. He, S.M. Njoroge, D. Wang, R. Shao, P. Lan, P. Lu, Ann. Phys. **532**, 1900570 (2020)
11. D.H. Ko, K.T. Kim, J. Park, J.-H. Lee, C.H. Nam, New J. Phys. **12**, 063008 (2010)
12. K. Kovacs, V. Tosa, Opt. Express **27**, 21873 (2019)
13. Z. Chang, Opt. Express **26**, 33238–33244 (2018)
14. R. Lopez-Martens, K. Varju, P. Johnsson, J. Mauritsson, Y. Mairesse, P. Salieres, M.B. Gaarde, K.J. Schafer, A. Persson, S. Svanberg, C.G. Wahlstrom, A. L'Huillier, Phys. Rev. Lett. **94**, 033001 (2005)
15. E. Gustafsson, T. Ruchon, M. Swoboda, T. Remetter, E. Pourtal, R. Lopez-Martens, P. Balcou, A. L'Huillier, Opt. Lett. **32**, 1353–1355 (2007)
16. D.H. Ko, K.T. Kim, C.H. Nam, J. Phys. B: At. Mol. Opt. Phys. **45**, 074015 (2012)
17. S.L. Cousin, N. Di Palo, B. Buades, S.M. Teichmann, M. Reduzzi, M. Devetta, A. Kheifets, G. Sansone, J. Biegert, Phys. Rev. X **7**, 041030 (2017)
18. A. Guggenmos, Y. Cui, S. Heinrich, U. Kleineberg, Appl. Sci. **8**, 2503 (2018)
19. A.-S. Morlens, R. Lopez-Martens, O. Boyko, P. Zeitoun, P. Balcou, K. Varju, E. Gustafsson, T. Remetter, A. L'Huillier, S. Kazamias, J. Gautier, F. Delmotte, M.-F. Ravet, Opt. Lett. **31**, 1558 (2006)
20. A. Wonisch, U. Neuhaeusler, N.M. Kabachnik, T. Uphues, M. Uiberacker, V. Yakovlev, F. Krausz, M. Drescher, U. Kleineberg, U. Heinzmann, Appl. Optics **45**, 4147 (2006)
21. M. Hofstetter, M. Schultze, M. Fiess, B. Dennhardt, A. Guggenmos, J. Gagnon, V.S. Yakovlev, E. Goulielmakis, R. Kienberger, E.M. Gullikson, F. Krausz, U. Kleineberg, Opt. Express **19**, 1767 (2011)
22. C. Bourassin-Bouchet, S. de Rossi, J. Wang, E. Meltchakov, A. Giglia, N. Mahne, S. Nannarone, F. Delmotte, New J. Phys. **14**, 023040 (2012)
23. C. Bourassin-Bouchet, Z. Diveki, S. de Rossi, E. English, E. Meltchakov, O. Gobert, D. Guénot, B. Carré, F. Delmotte, P. Salières, T. Ruchon, Opt. Express **19**, 3809–3817 (2011)
24. C. Bourassin-Bouchet, S. de Rossi, F. Delmotte, *Optical technologies for extreme-ultraviolet and soft X-ray coherent sources* (Springer, Berlin, Heidelberg, 2015)
25. A. Guggenmos, R. Rauhut, M. Hofstetter, S. Hertrich, B. Nickel, J. Schmidt, E.M. Gullikson, M. Seibald, W. Schnick, U. Kleineberg, Opt. Express **21**, 21728 (2013)
26. A. Guggenmos, S. Raduenz, R. Rauhut, M. Hofstetter, S. Venkatesan, A. Wochnik, E.M. Gullikson, S. Fischer, B. Nickel, C. Scheu, U. Kleineberg, Opt. Express **22**, 26526 (2014)
27. Y. Wang, B. Li, Nucl. Instrum. Methods Phys. Res. Sect. A **1001**, 165233 (2021)
28. C. Lin, S. Chen, D. Liu, Y. Liu, IEEE Photonics J. **4**, 1281–1287 (2012)
29. Q. Huang, V. Medvedev, R. van de Kruijs, A. Yakshin, E. Louis, F. Bijkerk, Appl. Phys. Rev. **4**, 011104 (2017)
30. V.N. Polkovnikov, S.A. Garakhin, D.S. Kvashennikov, I.V. Malyshev, N.N. Salashchenko, M.V. Svechnikov, R.M. Smertin, N.I. Chkhalo, Tech. Phys. **65**, 1809 (2020)
31. M.M. Barysheva, S.A. Garakhin, S.Y. Zuev, V.N. Polkovnikov, N.N. Salashchenko, M.V. Svechnikov, N.I. Chkhalo, S. Yulin, Quantum Electron. **49**, 380 (2019)
32. M.M. Barysheva, S.A. Garakhin, A.O. Kolesnikov, A.S. Pirozhkov, V.N. Polkovnikov, E.N. Ragozin, A.N. Shatokhin, R.M. Smertin, M.V. Svechnikov, E.A. Vishnyakov, Opt. Mater. Express **11**, 3038 (2021)
33. Y. Yao, H. Kunieda, Z. Wang, Opt. Express **21**, 8638 (2013)
34. T. Yang, S. Chen, C. Lin, J. Optics **24**, 045001 (2022)
35. S. Yang, S. Chen, C. Lin, J. Synchrotron Radiat. **28**, 1437 (2021)
36. A. Morlens, P. Balcou, P. Zeitoun, C. Valentin, V. Laude, S. Kazamias, Opt. Lett. **30**, 1554–1556 (2005)
37. M. Schultze, E. Goulielmakis, M. Uiberacker, M. Hofstetter, J. Kim, D. Kim, F. Krausz, U. Kleineberg, N. J. Phys. **9**, 243 (2007)
38. B.A.C. Castillo, J.S. Perez-Huerta, J. Madrigal-Melchor, S. Amador-Alvarado, I.A. Sustaita-Torres, V. Agarwal, D. Ariza-Flores, J. Appl. Phys. **127**, 203106 (2020)
39. B.L. Henke, E.M. Gullikson, J.C. Davis, At. Data Nucl. Data Tables **54**, 181 (1993)
40. I.L. Beigman, A.S. Pirozhkov, E.N. Ragozin, JETP Lett. **74**, 149–153 (2001)
41. N. Matuschek, L. Gallmann, D.H. Sutter, G. Steinmeyer, U. Keller, Appl. Phys. B **71**(4), 509–522 (2000)
42. J. Bellum, E. Field, T. Winstone, D. Kletecka, Coatings **6**(4), 11 (2016)